



Distinct roles of theta and gamma rhythms in inter-areal interaction in human visual cortex revealed by cortico-cortical evoked potentials

Primate visual cortex is hierarchically organized with dense inter-areal projections [1]. Primary visual cortex (V1), as the first stage of visual cortical processing, communicates with lower visual cortex (LVC, i.e., V2 and V3) and higher visual cortex (HVC, visual areas higher than V3) through both feedforward and feedback interactions [2,3]. One appealing assumption about efficient neuronal communication is that various kinds of communications are implemented through distinct frequency channels. Nowadays, accumulating evidence supports this assumption by revealing that low- and high-frequency rhythms subserve feedback influence and feedforward propagation, respectively [4–6]. However, whether V1 communicates with LVC and HVC through distinct frequency channels is unknown.

During stereo-electroencephalogram (sEEG) monitoring of epileptic patients, clinicians usually deliver a transient electrical stimulation to one cortical site and record cortico-cortical evoked potentials (CCEPs) in other cortical sites to analyze the effective connectivity in pathological and functional networks [7,8]. Therefore, CCEP mapping provides a direct way to probe the neuronal propagation *in vivo* with a high spatio-temporal resolution, which is an appropriate way to analyze the frequency-resolved interactions in human visual cortex.

Here, we conducted visual evoked potential (VEP) and CCEP experiments in nine epileptic patients (3 females, 16–46 years old) who underwent invasive sEEG monitoring for potential surgical treatments (Table S1). Only electrode contacts localized in occipital cortex were analyzed. All experimental procedures were approved by the Ethics Committee of the Sanbo Hospital of Capital Medical University and the Human Subject Review Committee of Peking University.

We first performed the VEP experiment and identified 100 visually responsive contacts in visual cortex (V1: $n = 47$; LVC: $n = 24$; HVC: $n = 29$; Fig. 1A and **Supplementary Methods**) [9]. In the CCEP experiment, we delivered trains of electrical biphasic pulses to pairs of adjacent visually responsive contacts (square-wave, 4 or 6 mA, 1 Hz, 200- μ s pulse width, 20 or 40 trials) and recorded sEEG signals simultaneously using a bipolar montage (Fig. 1B). During the CCEP experiment, patients were required to lie in bed with their eyes open. No visual stimulus was presented. No perceived phosphene was reported by the patients, indicating that the stimulation intensity was subthreshold for perception. We extracted significant CCEPs from the recorded sEEG signals of visually responsive contact pairs (**Supplementary Methods**). Thus, we obtained a total of 165 significant CCEPs (V1 \rightarrow LVC, feedforward, $n = 35$; LVC \rightarrow V1, feedback, $n = 31$; V1 \rightarrow HVC, feedforward, $n = 74$; HVC \rightarrow V1, feedback, $n = 25$) (Table S1).

We analyzed the post-stimulation powers of CCEPs in different frequency channels. For each CCEP, time-frequency components were extracted using the Morlet wavelet method (7 cycles, center frequency range: 2–150 Hz; frequency step: 1 Hz). The powers of the post-stimulation components (100–500 ms) were then averaged across trials and transformed into z-scores relative to the baseline (–200 to –100 ms; see Fig. 1C and D for examples). To be noted, we excluded the time period from –100 to 100 ms in the time-frequency analysis to avoid potential stimulation artifacts. The z-scored post-stimulation power changes were further averaged across time and binned into four frequency bands (theta: 4–8 Hz; alpha: 8–12 Hz; beta: 12–30 Hz; gamma: 30–60 Hz).

We first explored post-stimulation power changes of the CCEPs between V1 and LVC. As shown in Fig. 1E, no significant post-stimulation power change in the theta, alpha, or beta band in either feedforward or feedback condition was found (all $p > 0.05$, one-sample t-tests against zero). In the gamma band, the power change was significantly higher than the baseline in the feedback condition ($t(30) = 2.684$, $p = 0.012$), but no significant power change was found in the feedforward condition ($t(34) = -1.421$, $p = 0.164$). Then we compared the power changes between the feedforward and feedback conditions. Only the power changes in the gamma band were significantly different between the feedforward and feedback conditions ($t(64) = -2.956$, $p = 0.004$, independent t-test). Together, these results demonstrate that V1 communicates with LVC mainly through the gamma band, with an enhanced feedback power.

Accordingly, we probed post-stimulation power changes of the CCEPs between V1 and HVC. As shown in Fig. 1F, significant post-stimulation power reductions in the theta ($t(30) = -2.235$, $p = 0.028$), alpha ($t(30) = -2.186$, $p = 0.032$), and beta ($t(30) = -3.765$, $p = 3.340 \times 10^{-4}$) bands in the feedforward condition were found. Interestingly, in the feedback condition, we found a significant power enhancement in the theta band ($t(30) = 3.632$, $p = 0.001$) but a significant power reduction in the beta band ($t(30) = -2.378$, $p = 0.026$). No significant power change in the gamma band was found in either the feedforward or the feedback condition. We then tested the power changes between the feedforward and feedback conditions and only found a significant difference in the theta band ($t(97) = -3.776$, $p = 2.747 \times 10^{-4}$). These results indicate that V1 communicates with HVC through low-frequency channels, manifested as enhanced feedback and suppressed feedforward in the theta band.

In sum, combining intracranial VEP and CCEP techniques in humans, our findings revealed that V1 communicated with LVC and HVC through high- and low-frequency rhythms, respectively. Specifically, the feedback connectivity from LVC to V1 was characterized by

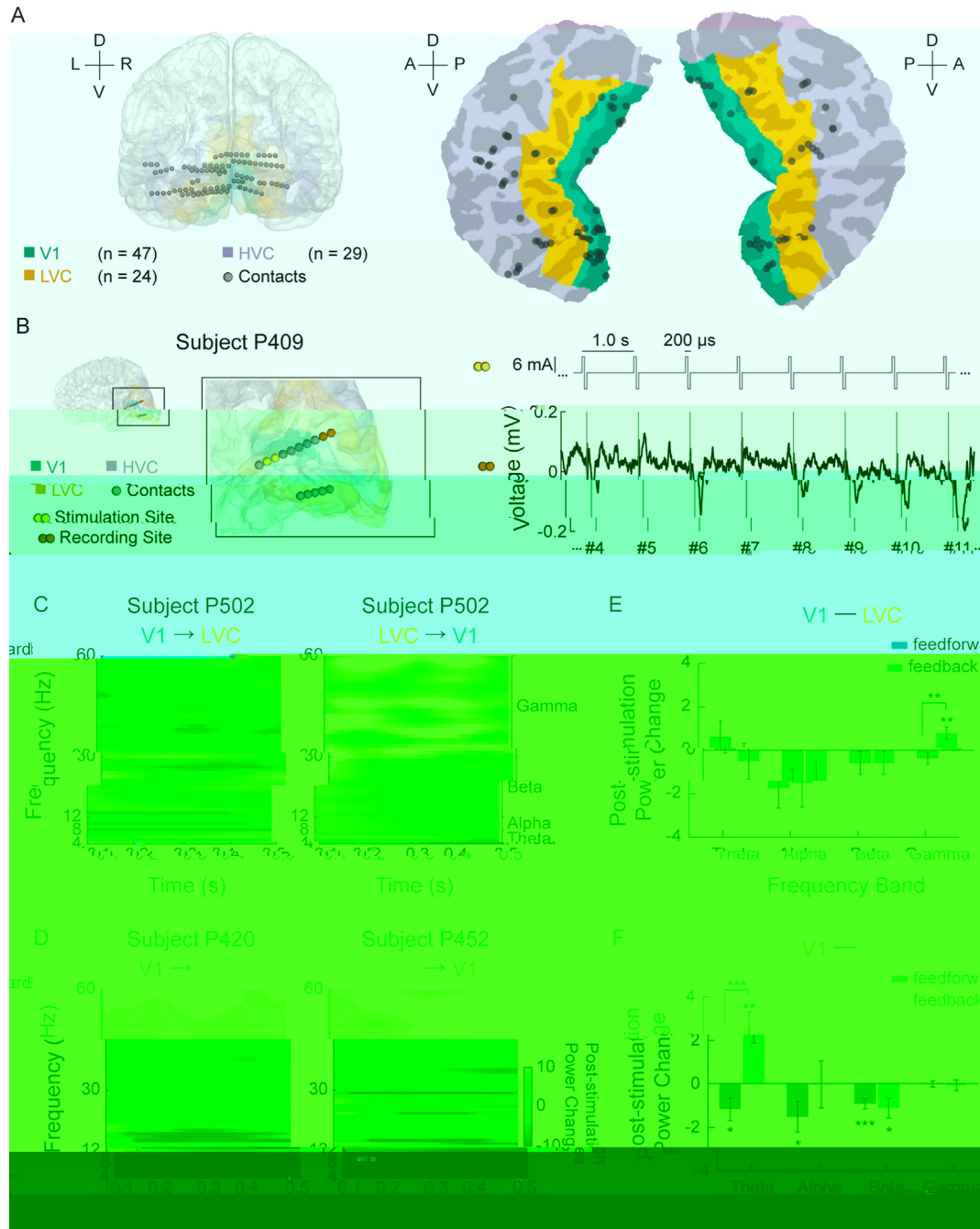


Fig. 1. (A) Locations of visually responsive sEEG contacts, visualized on a template brain (cvs_avg35_inMNI152, left) and a flattened occipital patch (right). The colors on the brain indicate different visual areas (green: V1; orange: LVC; purple: HVC). L: left; R: right; A: anterior; P: posterior; D: dorsal; V: ventral. (B) An example of electrical stimulation (upper right) and the raw sEEG signal (lower right; grey vertical lines: stimulation onsets) from the CCEP experiment. The stimulation (yellow) and recording (red) sites are visualized in the brain (subject P409, left). (C) Examples of post-stimulation time-frequency maps of CCEPs between V1 and LVC in the feedforward (left) and feedback (right) conditions. (D) Examples of post-stimulation time-frequency maps of CCEPs between V1 and HVC in the feedforward (left) and feedback (right) conditions. (E) Comparison of the post-stimulation power changes in each frequency band between V1 and LVC (blue: feedforward conditions; pink: feedback conditions). (F) Comparison of the post-stimulation power changes in each frequency band between V1 and HVC. Error bars: standard error; * $p < 0.05$;

an enhanced gamma-band power, while that from HVC to V1 was characterized by an enhanced theta band power. However, we only observed suppressed effects or no effect in the feedforward connectivity. Considering that we used transient and weak electrical pulses in the CCEP experiment, which did not induce any subjective visual experience for the patients, the suppression may reflect subthreshold neuronal activity. Overall, the current study provides direct evidence for the frequency-specific neuronal communication hypothesis in

humans, showing that gamma and theta rhythms subserve V1-LVC and V1-HVC functional connectivities, respectively [10].

Declaration of competing interest

The authors declare that they have no known competing financial interests or personal relationships that could have appeared to influence the work reported in this paper.

Acknowledgments

This work was supported by the National Science and Technology Innovation 2030 Major Program (2022ZD0204802, 2022ZD0204804) and the National Natural Science Foundation of China (31930053, 32171039) and Beijing Academy of Artificial Intelligence (BAAI).

Appendix A. Supplementary data

Supplementary data to this article can be found online at <https://doi.org/10.1016/j.brs.2022.07.056>.

References

- [1] Van Essen DC, Maunsell JH. Hierarchical organization and functional streams in the visual cortex. *Trends Neurosci* 1983;6:370–5.
- [2] Grill-Spector K, Malach R. The human visual cortex. *Annu Rev Neurosci* 2004;27(1):649–77.
- [3] Felleman DJ, Van Essen DC. Distributed hierarchical processing in the primate cerebral cortex. *Cerebr Cortex* 1991;1(1):1–47.
- [4] Bastos AM, Vezoli J, Bosman CA, Schoffelen J-M, Oostenveld R, Dowdall JR, et al. Visual areas exert feedforward and feedback influences through distinct frequency channels. *Neuron* 2015;85(2):390–401.
- [5] Michalareas G, Vezoli J, van Pelt S, Schoffelen J-M, Kennedy H, Fries P. Alpha-beta and gamma rhythms subserve feedback and feedforward influences among human visual cortical areas. *Neuron* 2016;89(2):384–97.
- [6] Van Kerkoerle T, Self MW, Dagnino B, Gariel-Mathis M-A, Poort J, Van Der Togt C, et al. Alpha and gamma oscillations characterize feedback and feedforward processing in monkey visual cortex. *Proc Natl Acad Sci USA* 2014;111(40):14332–41.
- [7] Keller CJ, Honey CJ, Mégevand P, Entz L, Ulbert I, Mehta AD. Mapping human brain networks with cortico-cortical evoked potentials. *Philos Trans R Soc Lond B Biol Sci* 2014;369(1653):20130528.
- [8] Lemaréchal J-D, Jedynak M, Trebaul L, Boyer A, Tadel F, Bhattacharjee M, et al. A brain atlas of axonal and synaptic delays based on modelling of cortico-cortical evoked potentials. *Brain* 2022;145(5):1653–67.
- [9] Yashor D, Bosking WH, Ghose GM, Maunsell JH. Receptive fields in human visual cortex mapped with surface electrodes. *Cerebr Cortex* 2007;17(10):2293–302.
- [10] Siegel M, Donner TH, Engel AK. Spectral fingerprints of large-scale neuronal interactions. *Nat Rev Neurosci* 2012;13(2):121–34.

Lu Luo

School of Psychology, Beijing Sport University, Beijing, 100084, China

Guanpeng Chen

School of Psychological and Cognitive Sciences and Beijing Key Laboratory of Behavior and Mental Health, Peking University, Beijing, 100871, China

IDG/McGovern Institute for Brain Research, Peking University, Beijing, 100871, China

Peking-Tsinghua Center for Life Sciences, Peking University, Beijing, 100871, China

Siqi Li

Shanghai Key Laboratory of Brain Functional Genomics (Ministry of Education), School of Psychology and Cognitive Science, East China Normal University, Shanghai, 200062, China

NYU-ECNU Institute of Brain and Cognitive Science at NYU Shanghai, Shanghai, 200062, China

Jing Wang

Department of Neurology, Sanbo Brain Hospital, Capital Medical University, Beijing, 100093, China

Qian Wang*

School of Psychological and Cognitive Sciences and Beijing Key Laboratory of Behavior and Mental Health, Peking University, Beijing, 100871, China

IDG/McGovern Institute for Brain Research, Peking University, Beijing, 100871, China

Fang Fang**

School of Psychological and Cognitive Sciences and Beijing Key Laboratory of Behavior and Mental Health, Peking University, Beijing, 100871, China

IDG/McGovern Institute for Brain Research, Peking University, Beijing, 100871, China

Peking-Tsinghua Center for Life Sciences, Peking University, Beijing, 100871, China

* Corresponding author.

** Corresponding author.

E-mail address: wangqianpsy@pku.edu.cn (Q. Wang).

E-mail address: ffang@pku.edu.cn (F. Fang).

14 July 2022

Available online 3 August 2022